Spin-dependent transport in nanocomposites of Alq3 molecules and cobalt nanoparticles

doi: 10.1063/1.2769748

Spin-dependent transport in nanocomposites of Alq_3 molecules and cobalt nanoparticles

Shinichi Tanabe, Shinji Miwa, Masaki Mizuguchi, Teruya Shinjo, Yoshishige Suzuki, and Masashi Shiraishi[a)]
Graduate School of Engineering Science, Osaka University, 1-3 Machikaneyama-cho, Toyonaka, Osaka 560-8531, Japan

(Received 30 December 2006; accepted 17 July 2007; published online 9 August 2007)

The authors have observed magnetoresistance (MR) ratios of 12% and 0.1% at 4.2 and 290 K, respectively, in a nanocomposite in which Co nanoparticles are embedded in the fine molecular structure of a tris(8-hydroxyquinoline) aluminum (Alq_3) matrix. Structural analyses, magnetization measurements, and conduction properties of the device reveal that the MR effect is induced by spin-dependent transport in the Alq_3. © *2007 American Institute of Physics*.
[DOI: 10.1063/1.2769748]

Spintronics is a field of electronics that utilizes both the charges and the spins of electrons, and it has been actively studied in order to fabricate spin-based devices.[1] Thus far, much effort has been devoted to applying metals and inorganic semiconductors to this field. Several groups[2–4] succeeded in observing the magnetoresistance (MR) effect in carbon nanotubes that were contacted by ferromagnetic electrodes, which demonstrated a potential use for molecules in spintronics. This concept of the so-called "molecular spintronics" should have an advantage over inorganic spintronics in terms of spin relaxation time, since a weak spin-orbit interaction is expected. Thus, introducing the use of molecules into the field of spintronics is a promising approach for manipulating electron spins and for fabricating spintronic devices with additional functions.

One of the most promising candidate materials for molecular spintronics is tris(8-hydroxyquinoline) aluminum (Alq_3), which has been demonstrated to exhibit efficient electroluminescence.[5] Alq_3-based spintronics studies focus on detecting spin-dependent transport through the MR effect[6] and circularly polarized light.[7] For instance, a high MR ratio of 40% at 11 K has been reported in a spin-valve device with a $Co/Alq_3/La_{1-x}Sr_xMnO_3$ sandwich structure.[6] However, the presence of an "ill-defined layer," i.e., a layer that may contain pinholes and Co inclusions in the Alq_3 layer, has impeded further investigation, such as a detailed structural analysis, and as yet, no MR effect has been observed at room temperature (RT). Hence, there is ample room for further investigation in this growing research field of Alq_3-based spintronics, and proposals for alternative approaches to manipulating electron spins in Alq_3 system could bring about further development.

A series of studies on C_{60}–Co nanocomposite systems,[8–10] where Co grains were dispersed in a C_{60} matrix, have verified that this system is suitable for observing spin-dependent transport by way of the MR effect in organic semiconductors. In particular, Miwa *et al.*[9] and Sakai *et al.*[10] have observed spin-dependent transport in C_{60}–Co nanocomposites up to RT and have also conducted structural analyses. The use of a Alq_3 matrix instead of a C_{60} matrix enables us to manipulate electron spins by utilizing both spin-dependent transport and spin-polarized luminescence. In this letter, we report the results of structural analysis and the observation of spin-dependent transport in Alq_3–Co nanocomposites.

We prepared 90-nm-thick Cr/Au electrodes on a glass substrate, in which the gap was 10 μm in length and 3 mm in width. Next, Alq_3 and Co (both of 99.99% purity) were coevaporated under high vacuum (10^{-5}–10^{-4} Pa) at a rate of 0.21 and 0.10 Å/s using an electron beam evaporator and a resistance heating evaporator, respectively. Thus, the concentration of Alq_3 to Co was 2.1:1.0 by volume. The total thickness of the Alq_3–Co layer was approximately 100 nm. A capping layer consisting of a 500 nm SiO layer and a 1.5 μm resist layer (ZEP-520A) was then deposited onto the Alq_3–Co layer to prevent the device from oxidizing. Finally, the sample was baked at 450 K for 30 min to solidify the resist layer. The device structure has been schematized elsewhere.[9] Attenuated total-reflection infrared (ATR-IR) spectroscopic analyses were conducted to verify that the Alq_3 maintained its structure after coevaporation. Magnetization measurements were performed to elucidate the Co grain structure and magnetization processes by using a superconducting quantum interference device. The electrical conduction characteristics were investigated by the two-terminal method using a source meter, and magnetic fields of up to 25 kOe were applied parallel to the electrical current using a cryostat equipped with superconducting solenoids.

Figure 1 shows the ATR-IR spectra of a quartz substrate, an evaporated Alq_3 film on a quartz substrate, and a coevaporated Alq_3–Co film on a quartz substrate, where the Alq_3 and the Co layers were prepared in the same manner, as mentioned above. The ATR-IR spectrum of the Alq_3 film exhibits the characteristic peaks of Alq_3, as shown in Ref. 11. The spectra of the coevaporated Alq_3–Co film and the Alq_3 film are very similar, although the peaks of the coevaporated film are slightly broader. This indicates that the Alq_3 molecules maintained their structure to a certain extent after coevaporation.

The magnetization curves at 4.2 and 290 K are shown in Fig. 2(a). At 4.2 K, hysteresis was observed around zero magnetic field, while no hysteresis was observed at 290 K. We also measured the time evolution of the residual magnetization of the device at 4.2 K and found that the residual

[a)]Electronic mail: shiraishi@mp.es.osaka-u.ac.jp

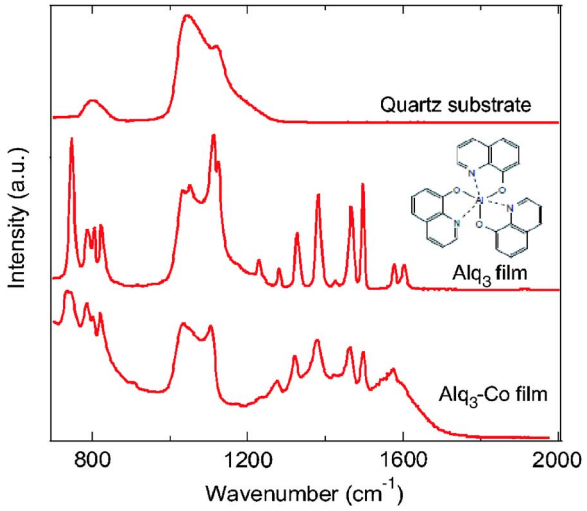

FIG. 1. (Color online) ATR-IR spectra of a quartz substrate, a Alq_3 film on a quartz substrate, and a Alq_3–Co film on a quartz substrate. The insert shows the molecular structure of Alq_3.

magnetization hardly changed with time. This suggests that the Alq_3–Co layer showed ferromagnetic behavior at 4.2 K and superparamagnetic behavior at 290 K. The diameter of the Co particles ranged from 2.4 to 3.7 nm, which was determined by fitting the *M-H* curve at 290 K to the Langevin function, taking the size distribution of the Co particles into account.

As shown in Fig. 2(b), the *I-V* characteristics at 4.2 K are nonlinear, suggesting the absence of percolation of Co granules between the electrodes. Our plot of $\log \rho$ vs $T^{-1/2}$ [see Fig. 2(c)] showed an approximately linear relationship, similar to that for a Co–Al–O insulating granular system.[12] In an insulating granular system, the conduction properties can be explained theoretically as hopping transport.[13] It is

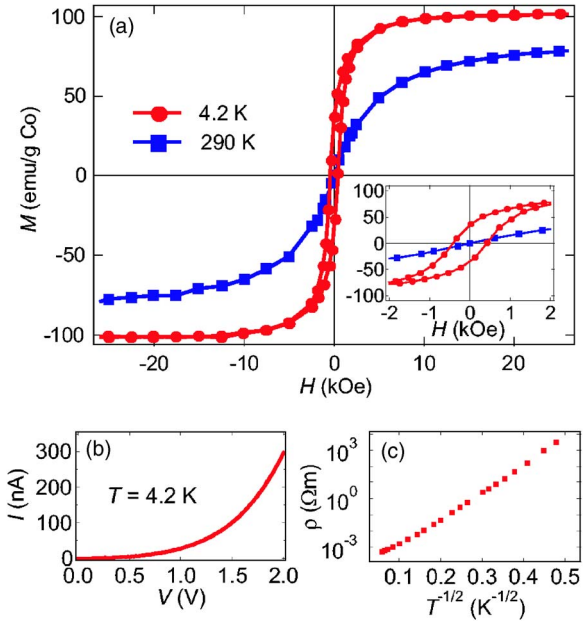

FIG. 2. (Color online) (a) Magnetization (M) as a function of magnetic field (H) for the Alq_3–Co nanocomposite at 4.2 and 290 K. The inset shows an expanded view of the plot near the origin. The lines are guides to the eye. (b) *I-V* characteristics of the Alq_3–Co nanocomposite at 4.2 K. (c) Temperature dependence of electrical resistivity (ρ) plotted as $\log \rho$ vs $T^{-1/2}$ for the Alq_3–Co nanocomposite at a bias voltage of 100 mV.

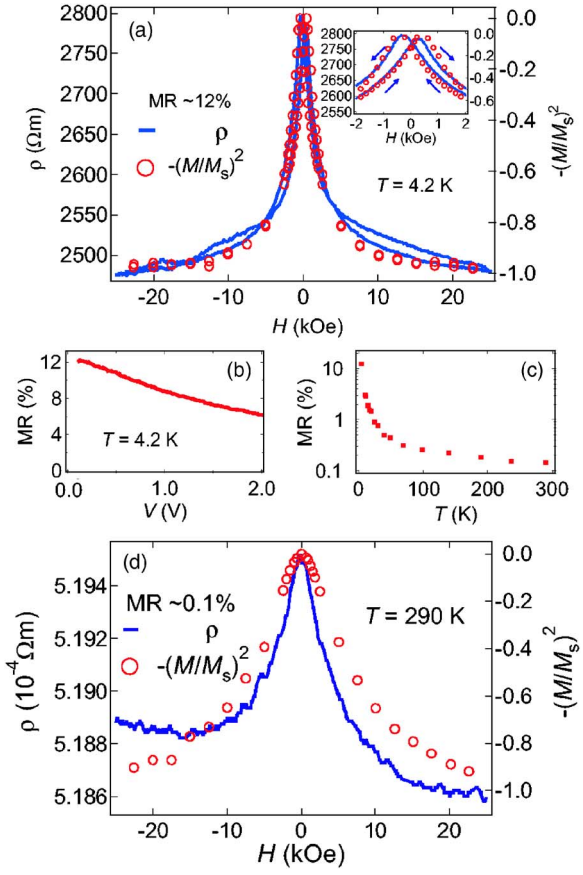

FIG. 3. (Color online) (a) Electrical resistivity (ρ) and $-(M/M_S)^2$ as a function of applied magnetic field (H) for the Alq_3–Co nanocomposite at 4.2 K for a bias voltage of 100 mV. The inset shows an expanded view of the plot near the origin. The arrows in the inset indicate the sweeping directions. (b) Bias voltage (V) dependence of the MR ratio at 25 kOe for the Alq_3–Co nanocomposite. The graph is derived from *I-V* curves at 0 and 25 kOe. (c) Temperature dependence of the MR ratio at a bias voltage of 100 mV for the Alq_3–Co nanocomposite. (d) Electrical resistivity (ρ) and $-(M/M_S)^2$ as a function of applied magnetic field (H) for the Alq_3–Co nanocomposite at 290 K and a bias voltage of 100 mV.

likely that the same conduction mechanism is in play in the Alq_3–Co nanocomposite, i.e., that the Alq_3 molecules behave as a tunneling barrier.

The MR curve at 4.2 K is shown in Fig. 3(a). It should be noted that hysteresis is observed around zero magnetic field, and the peak of the curve (~400 Oe) corresponds to the coercive force of the Co nanoparticles obtained from Fig. 2(a). If we define the MR ratio as $(\rho_{max}-\rho_{min})/\rho_{min}$, where ρ_{max} and ρ_{min} are the maximum and the minimum, respectively, then the MR ratio is calculated to be 12% at 4.2 K. The MR ratio of our device can be predicted theoretically as P^2, where P is the spin polarization of the ferromagnets. The derivation of this value, P^2, was implemented by modifying Julliere's model.[14] The conductivity (σ) in these models is proportional to $(1+P^2 \cos\theta)$, and $\cos\theta$ is proportional to $(M/M_S)^2$ in a nanocomposite (granular) system, where M and M_S are the global magnetization and the saturation magnetization, respectively. In addition, the value of $\cos\theta$ varies between 0 and 1 in a nanocomposite system because the "antiparallel state in spin alignment" refers to a randomly aligned state. Hence, $MR=(\rho_{max}-\rho_{min})/\rho_{min}=(\sigma_{min}^{-1}-\sigma_{max}^{-1})/\sigma_{max}^{-1}=[(1+P^2)-1]/1=P^2$. When $P=0.34$ is used as the value of spin polarization for Co,[15] the MR ratio is calculated to be about 12%, which agrees with the observed

results. In addition, $-(M/M_S)^2$ agrees well with ρ, as shown in Fig. 3(a). This relationship implies that electron conduction depends on the relative orientations of the magnetizations of the Co nanoparticles.[16] Figure 3(b) shows the bias voltage dependence of the MR ratio at 4.2 K, where the MR ratio decreases with increasing applied bias voltage. Although the MR ratio shows a comparatively weak bias voltage dependence, the temperature dependence of the MR ratio is rather strong, as shown in Fig. 3(c), However, we still observe a MR ratio of 0.1% and correspondence between ρ and $-(M/M_S)^2$ at 290 K [Fig. 3(d)]. The deviation of ρ and $-(M/M_S)^2$ at 290 K may be due to the size distribution of the Co nanoparticles. On the basis of the above discussion, the observed MR effects are attributed to spin-dependent transport in the Alq_3. Recently, another MR effect was reported[17] for devices where only Alq_3 was sandwiched between nonmagnetic electrodes. It should be noted that the cause of the MR effect in our system is completely different from that in Ref. 17. The spin-dependent transport in our system leads to different characteristics from those in Ref. 17 in terms of the temperature dependence of the MR ratio, for example.

It is noteworthy that the strong temperature dependence of the MR ratio cannot be explained by the temperature dependence of the saturation magnetization of the Co nanoparticles. Between 4.2 and 290 K, the decrease in the magnetization is about 20%, while the decrease in the MR ratio spans two orders of magnitude. The sharp change in the MR ratio may be due to a spin-flip process induced by the interaction of Alq_3 molecules and Co cluster surfaces. In addition, carrier injection from the Co nanoparticles to the Alq_3 may cause spin-flipping in the high-temperature region. Further studies are needed to explain the temperature dependence of the MR ratio in Alq_3–Co nanocomposites.

In summary, we have observed spin-dependent transport through the MR effect in Alq_3–Co nanocomposite device, where the Co nanoparticles were embedded in Alq_3 matrix. We have conducted structural analyses and studied the conduction properties. The MR ratio was 12% at 4.2 K and 0.1% at 290 K, and it was verified that the cause of the MR effect was spin-dependent transport between the Co nanoparticles in the Alq_3 matrix. The results obtained provide a basis for discussion of the underlying physics of the temperature dependence of the MR ratio in Alq_3-based spin devices.

The authors would like to thank the Low Temperature Center at Osaka University and S. Morimoto for their assistance in the magnetization measurements, and the Shimadzu Corporation for the ATR-IR measurements. The authors are also grateful to S. Nishioka and H. Tomita for their assistance in the MR measurements. This work was supported in part by the Asahi Glass Foundation.

[1] S. A. Wolf, D. D. Awschalom, R. A. Buhrman, J. M. Daughton, S. von Molnár, M. L. Roukes, A. Y. Chtchelkanova, and D. M. Treger, Science **294**, 1488 (2001).
[2] K. Tsukagoshi, B. W. Alphenaar, and H. Ago, Nature (London) **401**, 572 (1999).
[3] S. Sahoo, T. Kontos, J. Furer, C. Hoffmann, M. Gräber, A. Cottet, and C. Schöenenberger, Nat. Phys. **1**, 99 (2005).
[4] N. Tombros, S. J. van der Molen, and B. J. van Wees, Phys. Rev. B **73**, 233403 (2006).
[5] C. W. Tang and S. A. VanSlyke, Appl. Phys. Lett. **51**, 913 (1987).
[6] Z. H. Xiong, D. Wu, Z. V. Vardeny, and J. Shi, Nature (London) **427**, 821 (2004).
[7] E. Shikoh, A. Fujiwara, Y. Ando, and T. Miyazaki, Jpn. J. Appl. Phys., Part 1 **45**, 6897 (2006).
[8] H. Zare-Kolsaraki and H. Micklitz, Eur. Phys. J. B **40**, 103 (2004).
[9] S. Miwa, M. Shiraishi, M. Mizuguchi, T. Shinjo, and Y. Suzuki, Jpn. J. Appl. Phys., Part 2 **45**, L717 (2006).
[10] S. Sakai, K. Yakushiji, S. Mitani, K. Takanashi, H. Naramoto, P. V. Avramov, K. Narumi, V. Lavrentiev, and Y. Maeda, Appl. Phys. Lett. **89**, 113118 (2006).
[11] M. D. Halls and R. Aroca, Can. J. Chem. **76**, 1730 (1998).
[12] S. Mitani, S. Takahashi, K. Takanashi, K. Yakushiji, S. Maekawa, and H. Fujimori, Phys. Rev. Lett. **81**, 2799 (1998).
[13] P. Sheng, B. Abeles, and Y. Arie, Phys. Rev. Lett. **31**, 44 (1973).
[14] M. Julliere, Phys. Lett. **54A**, 225 (1975).
[15] P. M. Tedrow and R. Meservey, Phys. Rev. B **7**, 318 (1973).
[16] J. Q. Xiao, J. S. Jiang, and C. L. Chien, Phys. Rev. Lett. **68**, 3749 (1992).
[17] Ö. Mermer, G. Veeraraghavan, T. L. Francis, and M. Wohlgenannt, Solid State Commun. **134**, 631 (2005).